Infrared Spectroscopy And Elastic Properties Of Pr^{3+} Ions On Doped Co-Ni Ferrite

[1]D .V. Fugate., A. B. Kadam2*

[1] Department of Physics, Shivaji College, OmergaDist: Osmanabad (M.S.) India

*[2]Department of Physics,Jawahar Arts Science & Commerce College,

AnudurTq.Tuljapur,Dist.Osmanabad–413603

*Corresponding author: E-mail: drabkadam@gmail.com

Abstract:

Spinel ferrite system $Co_{0.6}Ni_{0.4}Fe_{2-x}Pr_xO_4$ (x = 0.000 to 0.100 in the step of 0.025) was prepared by sol-gel auto combustion method. The Fourier Transform Infrared Spectra (FT–IR) of the Co-Ni ferrite system have been analyzed at room temperature in between the frequency range of 200–800 cm^{-1}. The high-frequency absorption band 'υ_1' assigned to tetrahedral complex and low-frequency absorption band 'υ_2' assigned to octahedral complex. The force constant, bond length and Debye temperature were determined by infrared spectra analysis. The force constant, lattice constant and pore fraction have been used to investigate the elastic moduli such as Young's Modulus, Bulk Modulus, Rigidity Modulus.

Keywords: Co-Ni Ferrite, Infrared Spectroscopy, Elastic Property.

1.Introduction:

Ferrites Importance in basic as well as in applied research has been studied extensively [1].Co-Ni ferrite [2-4]Infra-red spectroscopy technique is based upon the chemical substance absorption in the infrared region. The functional group and bonds for the chemical substance form bands split in IR spectrum [5-9]. The infra-red spectroscopy (IR) is used to the study of various absorption bands in the spectrum, local symmetry, ordering phenomena, and elastic modulus, Debye temperature. The IR spectra analysis the spinel lattice and force constant split on the basis of cations present on tetrahedral [A] and octahedral [B] sites [10]. The ferrite system the inter-atomic and inter ionic-forces in solids are important in the understanding of the study of elastic properties [11]. The elastic constant
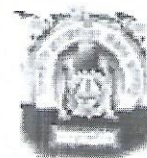
is important because of them elucidates the nature of the binding forces in the solid. The elastic modulus represents the mechanical strength fracture toughness and thermal stock resistance [12-14].

The nano ferrite $Co_{0.6}Ni_{0.4}Pr_xFe_{2-x}O_4$ (x = 0.0,0.025,0.05,0.075,0.1) were synthesized by Sol-gel Auto-Combustion method and also examine the effect of Pr^{3+}ions substitution in Co-Ni ferrites on the infra-red spectra and study of their elastic properties.

2.Experimental :

The nanocrystalline Pr^{+3}ions substitution Co-Ni ferrite having chemical composition $Co_{0.6}Ni_{0.4}Fe_{2-x}Pr_xO_4$(x=0.000, 0.025, 0.050, 0.075, 0.10).Synthesized by Sol-gel auto–combustion method[15].The infrared spectra of all the samples were recorded at room temperature in the range 200 to 800 cm^{-1} using Perkin Elmer infrared spectrophotometer.

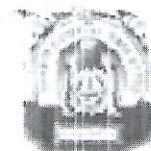## 3. Result and discussion:

3.1 Xrd:

The XRD patterns Fig.1 $Co_{0.6}Ni_{0.4}Fe_{2-x}Pr_xO_4$ (x=0.000, 0.025, 0.050, 0.075, 0.10). The observed peaks (220), (311), (222), (400), (422), (333) and (440) confirmed the formation of single phase cubic spinel and some secondary phase with increasing the Pr^{3+} ions contents. Shown in the fig.1. The secondary phase was identified to be orthoferrite phase of $PrFeO_3$. The lattice parameter 'a' was calculated using the following equation. [1]

$$a = d\sqrt{(h^2 + k^2 + l^2)}$$
(1)

Where, d is the inter-planer spacing and (hkl) is the index of the XRD reflection peak. It is observed from Table1. that lattice constant 'a' increased from 8.364Å to 8.412Å with an increase in Pr^{3+}ion substitution.

3.2 Infra-red Spectroscopy:

The IR spectrum in the range 200-800 cm^{-1} for nanocrystalline $Co_{0.6}Ni_{0.4}Pr_xFe_{2-x}O_4$ (x=0.000, 0.025, 0.050, 0.075, 0.10) ferrite system is illustrated in Fig.2. The observed variation in absorption bands for the present investigated system is listed in Table 1. IR spectrum of the synthesized samples displayed two absorption bands characteristic of the Spinel ferrites at 560-580 and 356-430 cm^{-1}. The higher frequency band (v_1) was due to the

Principal

Jawahar Arts, Science & Commerce College,
Andur Tal Tuljapur Dist. Osmanabad

stretching vibration of the tetrahedral metal-oxygen bond and the lower frequency band (v_2) was due to the octahedral metal-oxygen bond [5].

The band positions for all the investigated composition are given in Table 1. The change in the lattice constant is responsible for this shift of the center frequencies. The increase in the unit cell dimensions due to the replacement of Fe^{3+} ions by larger ionic radius Pr^{3+} ions affects the Fe^{3+}–O^{2-} stretching vibrations and this is a prominent cause of change in band positions. The change in the frequency of v_1 stretching band indicates the preference of Pr^{3+} ions to occupy the octahedral sites. The peak intensity of frequency bands slightly changes with an increasing Pr^{3+} substitution. It is known that the intensity ratio is a function of the change of dipole moment with the inter-nuclear distance ($d\mu/dr$) [12]. This value represents the contribution of the ionic bond Fe-O in the lattice. Furthermore, it is observed from Fig.2.That the normal mode of vibration of the tetrahedral cluster (v_1) is higher than that of an octahedral cluster(v_2), which is attributed to the shorter bond length of the tetrahedral cluster and longer bond length of octahedral cluster.
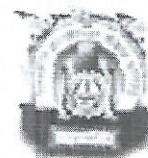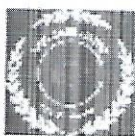
The bond lengths R_A and R_B have been calculated using the formula given by Gorter [16].

$$R_A = \left(u - \frac{1}{4}\right)a_{th}\sqrt{3} - R_o \tag{2}$$

$$R_B = \left(\frac{5}{8} - u\right)a_{th} - R_o \tag{3}$$

The values bond lengths for tetrahedral A-site (R_A) and octahedral B-site (R_B) were calculated and are given in Table 1. The bond length R_A and R_B increase with an increase in the composition of Pr^{3+} ion content. Increase in the lattice constant by the increasing value of x; this is in coherence with the bigger ionic radii of Pr^{3+} ions, which has been replaced by a smaller one for the Fe^{3+} ions. [17]. Using the analysis of Waldron [5], the force constant K_0 and K_t were calculated. According to Waldron the force constant K_t and K_o for respective sites are given by:

Our Heritage(UGC Care Listed)

ISSN: 0474-9030 Vol-68, Special Issue-2

National Conference on Recent Trends in Physics Chemistry and
Mathematics(RTPCM 2020) Held on 4th February 2020 Organised by
Department of Physics, Chemistry and Mathematics,
Sunderrao Solanke Mahavidhyalaya, Majalgaon, MS

$$K_t = 7.62 \times M_1 \times v_1^2 \times 10^{-3} \tag{4}$$

$$K_0 = 10.62 \times \frac{M_2}{2} \times v_2^2 \times 10^{-3} \tag{5}$$

Where, K_0 = force constant on octahedral site, K_t = force constant on tetrahedral site, M_1=Molecular weight of tetrahedral site, M_2=Molecular weight of octahedral site, v_1=Corresponding center frequency on tetrahedral site, v_2 = Corresponding center frequency on octahedral site. The values of forces are summarized in Table.1. The force constant K_o decreasing with the increasing Pr^{3+} content whereas K_t increases with the increase in Pr^{3+}. This variation can be related to the difference in ionic radii of Fe^{3+} and Pr^{3+} ions and their occupancy at A and B sites. Analysis of IR spectra with crystallographic knowledge helps us to determine the Debye temperature and elastic properties. The Debye temperature (θ_t) of all samples was calculated using the wave number of IR bands [5].
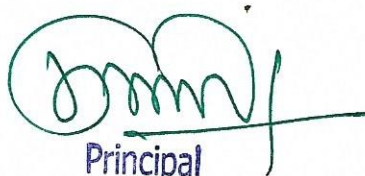
$$\theta l = hCVac/k \tag{6}$$

Where, h = $h/2\pi$, k is Boltzmann constant, C is the velocity of light (C = 3×10^8 cm/s) and V_{ac} is the average wave number of bands. Variation of Debye temperature with Pr^{3+} content is shown in Fig.3.

3.2 Elastic properties:

The elastic properties were determined using infrared spectroscopy [18-20] These elastic moduli were calculated using the values of lattice constant 'a', X-ray density 'd_x', pore fraction 'f' and force constant 'K'. Values of lattice constant, X-ray density and pore fraction are listed in Table 1. The average force constant (K) was calculated using the following relation:

$$k = kt + ko/2 \tag{7}$$

The bulk modulus of term stiffness constant C_{11} was calculated using relation [21-22]
Stiffness constant

$$C_{11} = \frac{K}{a} \qquad (8)$$

Where K is average force constant and a is lattice constant.

$$\text{Stiffness constant } (C_{12}) = \frac{\sigma \times C11}{(1-\sigma)} \qquad (9)$$

Where, σ is Poisson ratio and 'a' is the lattice constant. The Poisson ratio is function of

pore fraction ($\sigma = 0.324 \times 1 - 1.043f$).[23] Values of Poisson ratio are presented in Table 1. The Poisson ratio ranges in between 0.276 and 0.266, these values lie in the range of -1 to 0.5, which is in conformity with the theory of isotropic elasticity [12].

Variation of stiffness constants (C_{11} and C_{12}) as a function of Pr^{3+} content is shown in Fig.4.It is observed from both the stiffness constant decreased with increase in Pr^{3+} substitution. The values of Poisson's ratio were calculated using the relation discussed elsewhere [24].

The stiffness constant is affected by two factors; i.e. the tightness of bonding between the atoms and force constant. In present system bonds between Fe^{3+} and Pr^{3+} atoms are residual bond and due to this stiffness constant decrease with increasing Pr^{3+} content.These two stiffness constants are further used to calculate the various elastic constants such as; Young's modulus (E), bulk modulus (K) and modulus of rigidity (G).The other elastic moduli for the cubic structure are calculated using the following relation [12].

$$\text{Rigidity modulus } (G) = \frac{E}{2(\sigma +1)}$$

(10)

The rigidity modulus (G) is calculated using the relation 9 and the variation is presented in fig. 5.The values of modulus decreased with Pr^{3+} substitution. B, G, E decrease with increase in both Pr^{3+} it indicates that deformation of the solid is easy and the solid has less tendency to spring back to its equilibrium position. The Young's modulus, Bulk modulus and modulus of rigidity decrease with the increasing Pr^{3+} content. The decreases in elastic
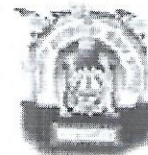
Moduli may be due to the interatomic binding between various atoms in the Spinel lattice. [20-25].

The inter-atomic bonding between the various atoms weakens continuously with the addition of Pr^{3+} content and therefore elastic moduli decrease with the increasing Pr^{3+} content. In Fe^{3+} $(3d^5)$ $Pr^{3+}(4f^3)$ ferrite repulsion between electrons may be increased with the increasing pr^{3+} content [5].

The longitudinal elastic wave velocity (V_L) and transverse (Shear) wave velocity (V_S) was calculated using the following equations,

$$\text{Longitudinal velocity} \quad V_L = \left(\frac{C_{11}}{\rho}\right)^{1/2}$$

(11)

$$\text{Transverse (Shear) velocity} \quad V_S = \left(\frac{G}{\rho}\right)^{1/2}$$

(12)

Where G is rigidity modulus with correct zero pore fraction. The values of V_l and V_s used to calculate mean wave velocity (V_m) which used to calculate Debye temperature was calculated using formula.[25]

$$\text{Debye temperature } \theta_E = \frac{h}{k}\left[\frac{3\rho q N_A}{4 \Pi M}\right]^{1/3} \times V_m$$

(13)

Where h is plank's constant, k is Boltzmann's constant, M is molecular weight, q is the number of an atom in the unit formula and V_m mean wave velocity.

$$\frac{3}{V_m^3} = \frac{1}{V_l^3} + \frac{2}{V_s^3}$$

(14)

The values of a longitudinal wave, shearing wave and mean wave velocity are calculated using relation10, 11 and13 respectively. It is observed from fig.6.the longitudinal elastic wave velocity is decreases whereas transverse (Shear) wave velocity increased with Pr^{3+} substitution. The values of wave velocities are similar to other ferrites those obtained from UPT method [26].

Our Heritage(UGC Care Listed)
ISSN:0474-9030 Vol-68, Special Issue-12

National Conference on Recent Trends in Physics, Chemistry and
Mathematics(RTPCM-2020) Held on 4th February 2020Organised by:
Department of Physics,Chemistry and Mathematics,
Sundarrao Solanke Mahavidhyalaya, Majalgaon, MS

The variation of Debye temperature (θ_E) calculated by using the relation 12. Given in Fig.3. the Debye temperature increased with Pr^{3+}substitution. It suggested that lattice vibrations are hindered due toPr^{3+}substitution. This may be due to the fact that the strength of inter atomic bonding increases with concentration [26].

The values of V_l/p and V_S/p are calculated by Anderson equation [27] shown in fig .7. the decrease with increasing Pr^{3+} ions substitution [18].

A plot of average sound velocity (V_m) against Debye temperature (θ_E) is shown in Fig .8. It is interesting to note from the figure that the average sound velocity increases linearly with the Debye temperature. This behaviour clearly indicates the direct relationship between the acoustic parameter (average sound velocity) and the important thermodynamic parameter Debye temperature [28-29].
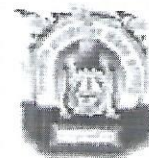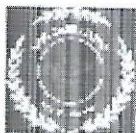
4.Conclusion:

The Pr^{3+} substituted $Co_{0.6}Ni_{0.4}Pr_xFe_{2-x}O_4$ ferrite nanoparticles were prepared by using the sol-gel auto-combustion method. IR spectra confirmed the formation of Spinel structure and gave information about the distribution of ions between the two sites, tetrahedral (A-site) at 575 cm^{-1} and octahedral (B-site) at 370 cm^{-1}. The Elastic properties such as elastic wave velocity, elastic constant and Debye temperature calculated using XRD and IR data. The elastic constants decreased with the increase in Pr^{3+} content. The elastic moduli and Debye Temperature are found to decreasing with increasing praseodymium
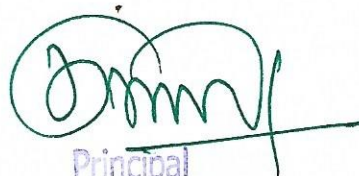
5. References:

1. Algude, S. G., Patange, S. M., Shirsath, S. E., Mane, D. R., & Jadhav, K. M. (2014). Elastic behavior of Cr^{3+} substituted Co–Zn ferrites. *Journal of Magnetism and Magnetic Materials, 350,* 39-41.

2. Kim, C. S., Lee, S. W., Park, S. I., Park, J. Y., & Oh, Y. J. (1996). Atomic migration in Ni-Co ferrite. *Journal of applied physics, 79*(8), 5428-5430.

3. Niu, Z. P., Wang, Y., & Li, F. S. (2006). Magnetic properties of nanocrystalline Co–Ni ferrite. *Journal of materials science, 41*(17), 5726-5730.

Principal
Jawahar Arts, Science & Commerce College,
Andur Tal. Tuljapur Dist, Osmanabad

Our Heritage(UGC Care Listed)

ISSN : 0474-9030 Vol-68, Special Issue-12

National Conference on Recent Trends in Physics Chemistry and
Mathematics(RTPCM-2020) Held on 4th February 2020Organized by:
Department of Physics, Chemistry and Mathematics
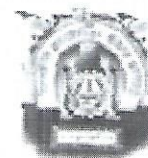Sunderrao Solanke Mahavidyalaya Majalgaon MS

4. Gao, Y., Zhao, Y., Jiao, Q., & Li, H. (2013). Microemulsion-based synthesis of porous Co–Ni ferrite nanorods and their magnetic properties. *Journal of Alloys and Compounds*, *555*, 95-100.

5. Waldron, R. D. (1955). Infrared spectra of ferrites. *Physical Review*, *99*(6), 1727.

6. Josyulu, O. S., &Sobhanadri, J. (1981). The far-infrared spectra of some mixed cobalt zinc and magnesium zinc ferrites. *Physica status solidi (a)*, *65*(2), 479-483.

7. Amer, M. A., Ahmed, M. A., El-Nimr, M. K., & Mostafa, M. A. (1995). Mossbauer and infrared studies of the Cu-Cr ferrites. *Hyperfine Interactions*, *96*(1), 91-98.

8. Pradeep, A., & Chandrasekaran, G. (2006). FTIR study of Ni, Cu, and Zn substituted nano-particles of $MgFe_2O_4$. *Materials Letters*, *60*(3), 371-374.

9. Rao, G. S., Rao, C. N. R., & Ferraro, J. R. (1970). Infrared and electronic spectra of rare-earth perovskites: ortho-chromites,-manganites and-ferrites. *Applied Spectroscopy*, *24*(4), 436-445.

10. Modi, K. B., Shah, S. J., Pujara, N. B., Pathak, T. K., Vasoya, N. H., &Jhala, I. G. (2013). Infrared spectral evolution, elastic, optical and thermodynamic properties study on mechanically milled $Ni_{0.5}Zn_{0.5}Fe_2O_4$ spinel ferrite. *Journal of Molecular Structure*, *1049*, 250-262.

11. Patange, S. M., Shirsath, S. E., Lohar, K. S., Algude, S. G., Kamble, S. R., Kulkarni, N., ... & Jadhav, K. M. (2013). Infrared spectral and elastic moduli study of $NiFe_{2-x}Cr_xO_4$ nanocrystalline ferrites. *Journal of Magnetism and Magnetic Materials*, *325*, 107-111.

12. Patil, V. G., Shirsath, S. E., More, S. D., Shukla, S. J., & Jadhav, K. M. (2009). Effect of zinc substitution on structural and elastic properties of cobalt ferrite. *Journal of Alloys and Compounds*, *488*(1), 199-203.

13. Lakhani, V. K., & Modi, K. B. (2010). Al^{3+}modified elastic properties of copper ferrite. *Solid-State Sciences*, *12*(12), 2134-2143.

14. Tatarchuk, T. R., Paliychuk, N. D., Bououdina, M., Al-Najar, B., Pacia, M., Macyk, W., &Shyichuk, A. (2018). Effect of cobalt substitution on structural, elastic, magnetic and optical properties of zinc ferrite nanoparticles. *Journal of Alloys and Compounds*, *731*, 1256-1266.

Principal
Jawahar Arts, Science & Commerce College,
Andur Tal. Tuljapur Dist, Osmanabad

Our Heritage(UGC Care Listed)

ISSN:0474-9030 Vol-68, Special Issue-12

National Conference on Recent Trends in Physics Chemistry and
Mathematics (RTPCM-2020) Held on 4th February 2020Organised by:
Department of Physics, Chemistry and Mathematics,
SunderraoSolankeMahavidhyalaya, Majalgaon, MS

15. Chen, D. H., & He, X. R. (2001). Synthesis of nickel ferrite nanoparticles by sol-gel method. *Materials Research Bulletin, 36*(7-8), 1369-1377.

16. Gorter, Evert Willem. *Philips Res. Rep.* 9 (1954): 295-320.

17. Lohar, K. S., Pachpinde, A. M., Langade, M. M., Kadam, R. H., &Shirsath, S. E. (2014). Self-propagating high-temperature synthesis, structural morphology and magnetic interactions in rare-earth Ho^{3+} doped $CoFe_2O_4$ nanoparticles. *Journal of Alloys and Compounds, 604*, 204-210.

18. Ravinder, D., Kumar, K. V., &Boyanov, B. S. (1999). Elastic behavior of Cu–Zn ferrites. *Materials Letters, 38*(1), 22-27.

19. Modi, K. B., Gajera, J. D., Pandya, M. P., Vora, G., & Joshi, H. H. (2004). Far-infrared spectral studies of magnesium and aluminum co-substituted lithium ferrites. *Pramana, 62*(5), 1173-1180.

20. Shirsath, S. E., Patange, S. M., Kadam, R. H., Mane, M. L., & Jadhav, K. M. (2012). Structure refinement, cation site location, spectral and elastic properties of Zn2+ substituted NiFe2O4. *Journal of molecular structure, 1024,* 77-83.

21. Pathak, T. K., Buch, J. J. U., Trivedi, U. N., Joshi, H. H., & Modi, K. B. (2008). Infrared spectroscopy and elastic properties of nanocrystalline Mg–Mn ferrites prepared by co-precipitation technique. *Journal of nanoscience and nanotechnology, 8*(8), 4181-4187.

22. Kakani, S. L., &Hemrajani, C. (1997). Textbook of solid-state physics. *Sultan Chand & Sons, New Delhi.*

23. Raj, V. B., & Palanichamy, P. R. (2004). Science and Technology of Ultrasonics, Narosa Publ. *House, New Delhi,* 250.

24. Bhatu, S. S., Lakhani, V. K., Tanna, A. R., Vasoya, N. H., Buch, J. U., Sharma, P. U.& Modi, K. B. (2007). Effect of nickel substitution on structural, infrared and elastic properties of lithium ferrite.

25. Wooster, W. A. (1953). Physical properties and atomic arrangements in crystals. *Reports on Progress in Physics, 16*(1), 62.

26. Mazen, S. A., &Elmosalami, T. A. (2012). Structural and elastic properties of Li-Ni ferrite. ISRN Condensed Matter Physics, 2011

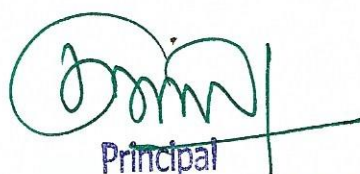27. Anderson, O. L., Mason, W. P., & Thurston, R. N. (1965). Physical Acoustics. Vol. III, Part B.

Our Heritage(UGC Care Listed)

ISSN: 0474-9030 Vol-68, Special Issue-12

National Conference on Recent Trends in Physics Chemistry and
Mathematics(RTPCM-2020) Held on 4th February 2020Organised by
Department of Physics, Chemistry and Mathematics
Sunderrao Solanke Mahavidhyalaya Majalgaon, MS

28. Reddy, P. V. (1988). High-temperature elastic behaviour of Mn-Mg mixed ferrites. *physica status solidi (a)*, 108(2), 607-611.

29. Revathi, M. B., & Rao, T. S. (1974). Elastic behavior of mixed cobalt-zinc ferrites. *Journal of the Less-Common Metals*, 34(1), 91-96.

Fig. 1: X-Ray diffraction patterns of $Pr_xCoFe_{2-x}O_4$. (x=0.0,0.025,0.050,0.075,0.1)
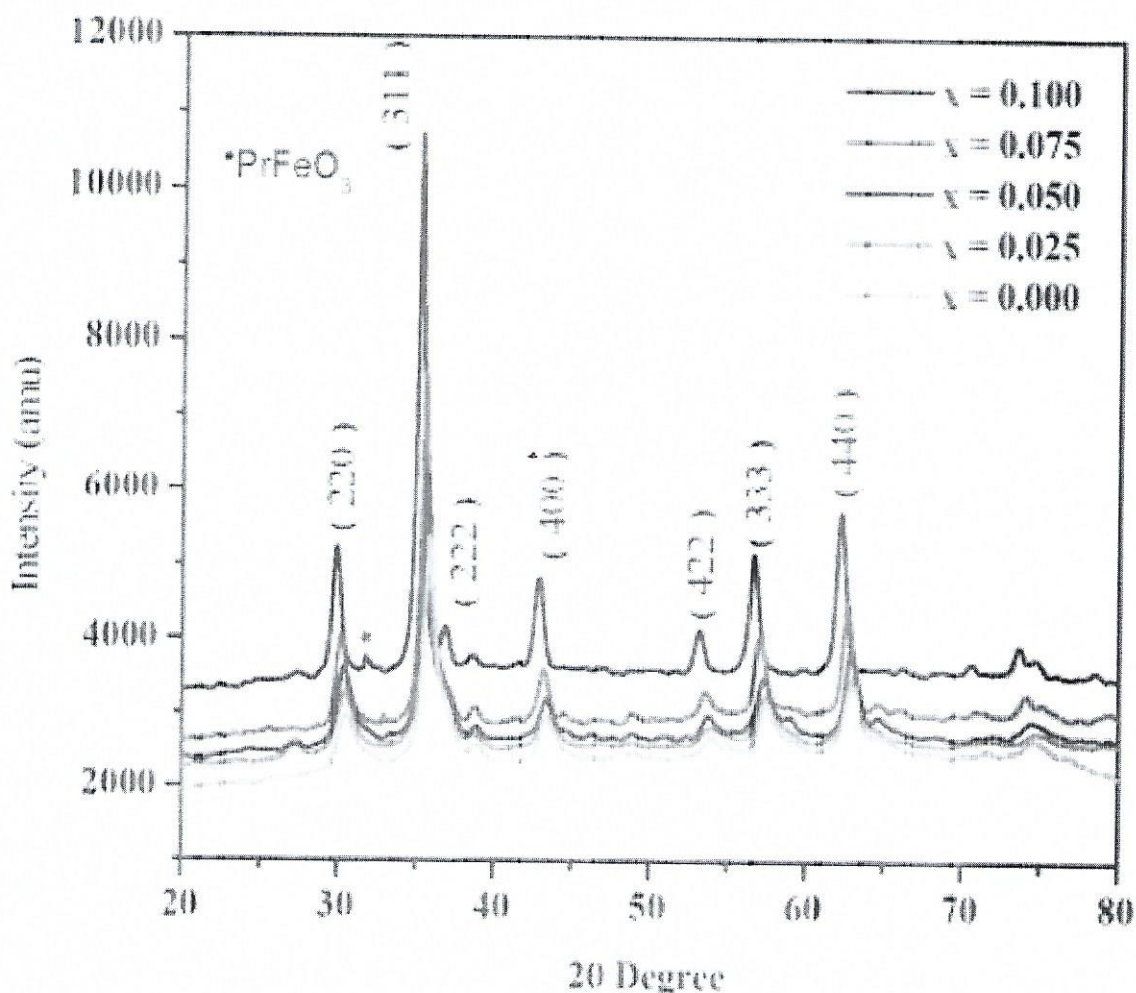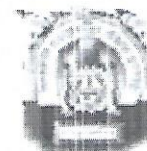
Fig.2 Infra red spectra of $Co_{0.6}Ni_{0.4}Fe_{2-x}Pr_xO_4$, (x=0.0,0.025,0.050,0.075,0.1)
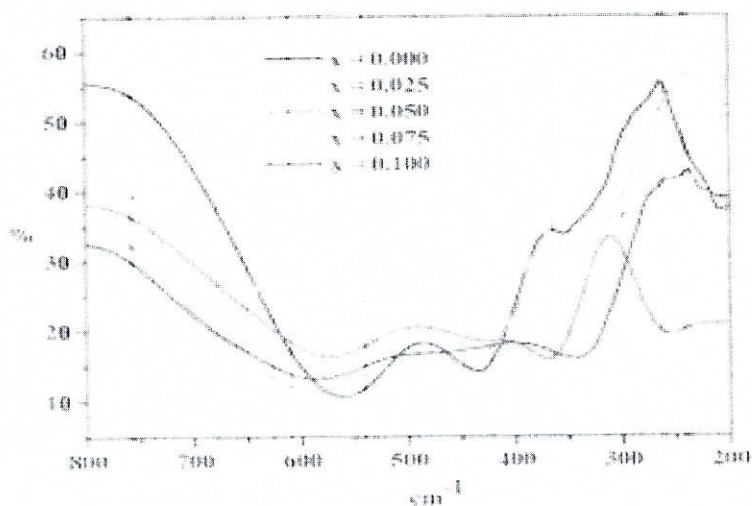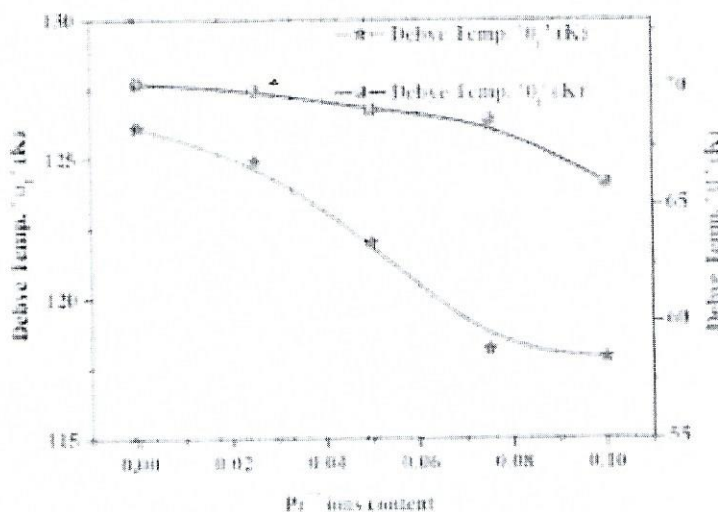

**Fig.3.Variation of Debye temperature calculated form infrared (θ_I) and elastic (θ_E)
with Pr^{3+} content.**

Principal
Jawahar Arts, Science & Commerce College,
Andur Tal. Tuljapur Dist, Osmanabad

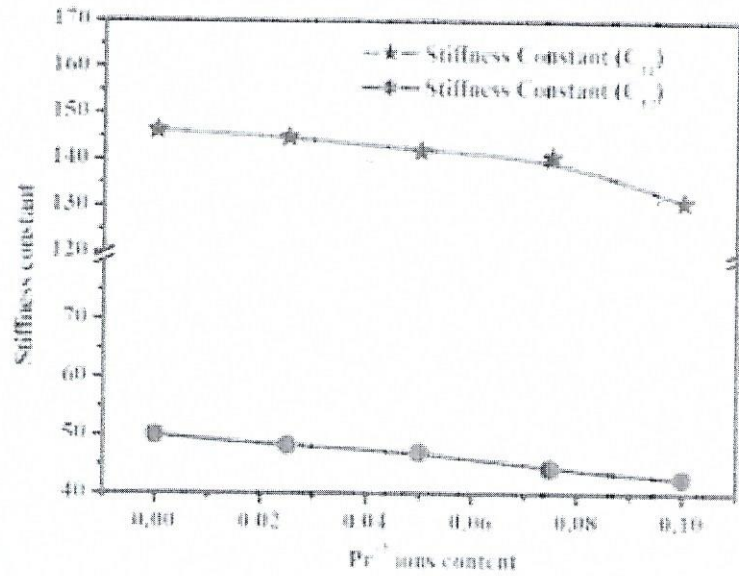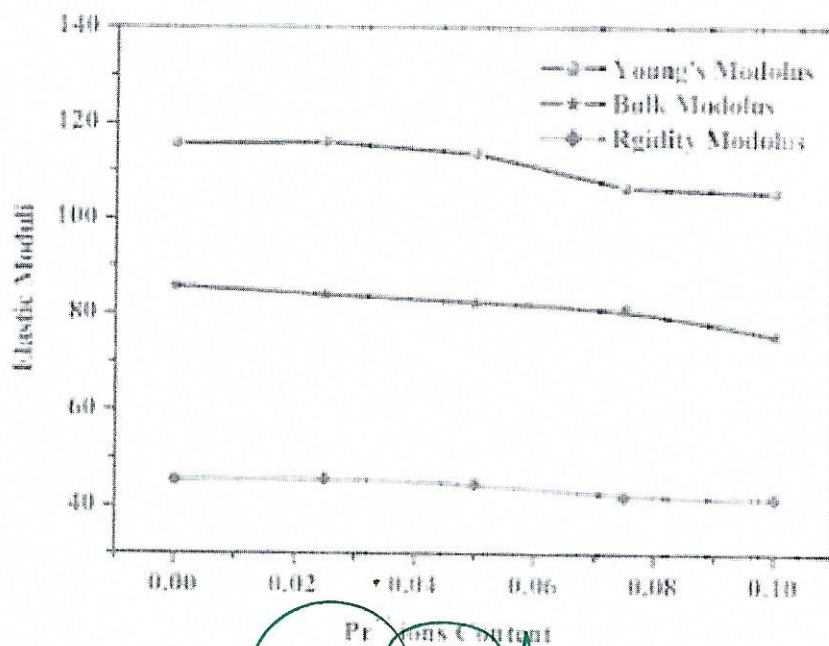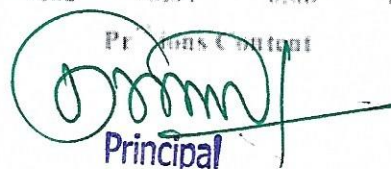**Fig.4. Variation of stiffness constants (C_{11} and C_{12}) with Pr^{3+} content.**

Fig.5. Variation of Young's modulus (E), bulk modulus (K) and modulus of rigidity(G) with Pr^{3+} content.

Principal
Jawahar Arts, Science & Commerce College,
Andur Tal. Tuljapur Dist. Osmanabad

Our Heritage(UGC Care Listed)

ISSN: 0474-9030 Vol-68, Special Issue-12

National Conference on Recent Trends in Physics, Chemistry and
Mathematics, RTPCM-2020, Held on 4th February 2020 Organised by:
Department of Physics, Chemistry and Mathematics,
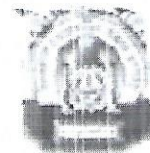Sunderrao Solanke Mahavidhyalaya, Majalgaon, MS

Fig.6. Variation of shearing velocity (V_S), mean wave velocity (V_m) and longitudinal wave velocity (V_L) with Pr^{3+} content.
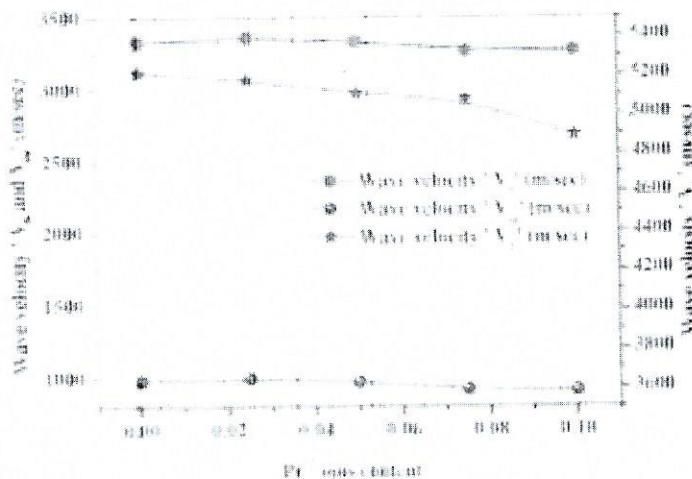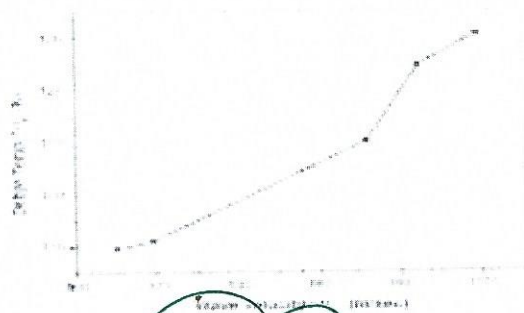

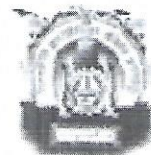**Fig.7. V_l/p and Vs/p against Pr^{3+} ion content.**

Fig. 8. Debye temperature θ_E against average sound velocity V_m.

Principal
Jawahar Arts, Science & Commerce College,
Andur Tal. Tuljapur Dist, Osmanabad

Table 1 Lattice constant 'a', X ray density 'dx', Bondlengths (R_A & R_B), Absorption bands (v_1 and v_2)Force constant 'K' and Poisson's ratio 'σ' of$Co_{0.6}Ni_{0.4}Fe_{2-x}Pr_xO_4$ (x = 0.000, 0.025, 0.050. 0.075, 0.100).

Comp. x	'a' (Å)	'd_x' (g/cm^3)	v_1 (cm^{-1})	v_2 (cm^{-1})	R_A (Å)	R_B (Å)	$K_t \times 10^5$ (dyne/cm)	$K_o \times 10^5$ (dyne/cm)	(K)= (K_t+K_o)	Poisson ratio σ
0.000	8.364	5.384	556	420	3.801	3.041	1.353	1.093	1.223	0.275
0.025	8.376	5.41	576	396	3.804	3.042	1.456	0.971	1.214	0.270
0.050	8.381	5.448	586	374	3.806	3.044	1.514	0.866	1.190	0.269
0.075	8.397	5.465	589	365	3.807	3.044	1.539	0.824	1.181	0.268
0.100	8.412	5.482	591	326	3.812	3.046	1.550	0.655	1.103	0.267

Principal
Jawahar Arts, Science & Commerce College,
Andur Tal. Tuljapur Dist. Osmanabad